Cancer Cell
Article

Tumor-Derived Jagged1 Promotes Osteolytic Bone Metastasis of Breast Cancer by Engaging Notch Signaling in Bone Cells

Nilay Sethi,[1,2] Xudong Dai,[3,5] Christopher G. Winter,[3] and Yibin Kang[1,4,*]
[1]Department of Molecular Biology, Princeton University, Princeton, NJ 08544, USA
[2]MD/PhD Program, Robert Wood Johnson Medical School, Piscataway, NJ 08903, USA
[3]Merck Research Laboratories, Boston, MA 02115, USA
[4]Breast Cancer Program, Cancer Institute of New Jersey, New Brunswick, NJ 08903, USA
[5]Present address: Sage Bionetworks, Seattle, WA 98109, USA
*Correspondence: ykang@princeton.edu
DOI 10.1016/j.ccr.2010.12.022

SUMMARY

Despite evidence supporting an oncogenic role in breast cancer, the Notch pathway's contribution to metastasis remains unknown. Here, we report that the Notch ligand Jagged1 is a clinically and functionally important mediator of bone metastasis by activating the Notch pathway in bone cells. Jagged1 promotes tumor growth by stimulating IL-6 release from osteoblasts and directly activates osteoclast differentiation. Furthermore, Jagged1 is a potent downstream mediator of the bone metastasis cytokine TGFβ that is released during bone destruction. Importantly, γ-secretase inhibitor treatment reduces Jagged1-mediated bone metastasis by disrupting the Notch pathway in stromal bone cells. These findings elucidate a stroma-dependent mechanism for Notch signaling in breast cancer and provide rationale for using γ-secretase inhibitors for the treatment of bone metastasis.

INTRODUCTION

The Notch-signaling pathway regulates a broad spectrum of cell-fate decisions during development and postnatal life (Artavanis-Tsakonas et al., 1999). The pathway is activated when a signal-sending cell expressing a Notch ligand physically interacts with a signal-receiving cell expressing a Notch receptor. Upon ligand binding, the transmembrane Notch receptor is cleaved sequentially, first by an extracellular matrix metalloprotease and then by the protease complex γ-secretase, releasing the Notch intracellular domain (N^{ICD}). After being liberated, N^{ICD} translocates to the nucleus where it interacts with the DNA-binding protein CSL (Rbp-Jκ in mice; CBF1 in humans), converting it from a transcriptional repressor to activator by recruiting cofactors such as Mastermind-like proteins. The most prominent targets of the Notch pathway include a set of basic-helix-loop-helix factors of the Hes and Hey families (Kopan and Ilagan, 2009).

Although classically known for its role in embryonic development, the Notch pathway is now being recognized for its aberrant activation in cancer. An oncogenic role for Notch was first discovered in T cell acute lymphoblastic leukemia (T-ALL), and then extended to other malignancies including lung, ovary, breast, and skin cancers (reviewed by Rizzo et al., 2008). Only recently has Notch signaling been associated with cancer progression; it was shown to regulate mediators of invasion in pancreatic cancer (Wang et al., 2006) and promote epithelial-mesenchymal transition (Leong et al., 2007). Interestingly, the Notch ligand Jagged1 is also associated with cancer progression because it is overexpressed in patients with poor prognosis prostate and breast cancer (Reedijk et al., 2005; Santagata et al., 2004). Despite these advances, the functional mechanism of the Notch pathway in breast cancer metastasis is poorly defined.

Bone metastasis affects over 70% of metastatic breast cancer with debilitating bone fractures, severe pain, nerve compression,

Significance

Although Notch pathway activation leads to tumorigenesis, little is known about the role of Notch signaling in metastasis. Here, we report that elevated expression of the Notch ligand Jagged1 is associated with breast cancer bone metastasis. Functional studies revealed that tumor-derived Jagged1 promotes osteolytic bone metastasis of breast cancer by activating the Notch pathway in the bone microenvironment. These findings establish a distinct paradigm for Notch signaling in breast cancer, as we define a requirement for the pathway in the supporting microenvironment of bone metastases rather than the tumor cells. Importantly, pharmacological inhibition of the Notch pathway in stromal bone cells reduced Jagged1-mediated bone metastasis and provided preclinical evidence for using γ-secretase inhibitors as therapeutic agents against bone metastasis.

and hypercalcemia (Mundy, 2002). The development and outgrowth of these secondary lesions depend on the intricate cellular and molecular interactions between breast tumor cells and stromal cells of the bone microenvironment. In particular, the ability of tumor cells to disrupt the bone homeostatic balance maintained by two resident bone cell types, osteoclasts and osteoblasts, has been shown to drive bone destruction and metastatic tumor growth (Mundy, 2002). Tumor cells secrete signaling proteins, such as parathyroid hormone-related peptide (PTHrP) (Guise et al., 1996), to promote osteoclast differentiation and activity, either directly or indirectly by altering osteoblast production of receptor activator of nuclear factor-κB ligand (RANKL), an essential osteoclast differentiation cytokine, and its antagonist osteoprotegerin (OPG). The resultant bone destruction releases a number of growth factors stored in the bone matrix, such as transforming growth factor-β (TGFβ), to further stimulate the malignancy of tumor cells, completing the so-called "vicious cycle" in bone metastasis. Although several molecular contributors of bone metastasis have been identified, effective therapies still await a more comprehensive understanding of the complex molecular and cellular network of tumor-stromal interactions in bone metastasis. In this study we investigated the role of Notch signaling in the development of osteolytic bone metastasis of breast cancer.

RESULTS

The Notch Ligand Jagged1 Is Associated with Breast Cancer Bone Metastasis

To investigate the potential role of Notch signaling in breast cancer metastasis, we evaluated the endogenous expression of pathway ligands, receptors, and downstream targets in the 4T1 series of mouse mammary tumor cell lines with increasing metastatic abilities (Aslakson and Miller, 1992). Although all of the cell lines in this series form primary tumors with similar growth kinetics, only 4T1 is capable of developing bone metastasis spontaneously (Lelekakis et al., 1999). Gene expression analysis of the Notch pathway receptors and prominent downstream targets revealed no association with metastatic ability (see Figures S1A and S1B available online). In contrast, Notch ligand levels were markedly elevated in the 4T1 cell line (Figure 1A; Figure S1C). Moreover, expression profiling of human MDA-MB-231 (MDA231) breast cancer sublines with distinct bone metastatic abilities (Kang et al., 2003) revealed that *JAGGED1* (*JAG1*) levels were significantly elevated in aggressive bone-tropic sublines compared to the weakly metastatic ones (Figure 1B; Figure S1D) ($p < 0.01$). These findings suggested a possible link between tumor expression of Notch ligands and breast cancer bone metastasis.

To determine the clinical significance of Jagged1 in breast cancer metastasis, we examined its expression pattern in tumor samples from patients in two previously reported data sets. The Wang data set (Wang et al., 2005) revealed that *JAG1* expression was significantly higher in patients with relapse ($p = 0.0045$, Student's t test). Moreover, incidence of relapse was significantly greater in patients with high *JAG1* expression compared to those with low expression (Figure 1C). In contrast the incidence of relapse was not significantly different in patients with low or high expression of *NOTCH1* or *HES1* (Figures S1E–S1G). Distinct from the Wang data set, the Minn data set (Minn et al., 2005) includes more diverse clinical criteria such as organ-specific metastasis. The incidence of bone metastasis was significantly greater in patients with high *JAG1* expression compared to those with low expression (Figure 1D). In contrast, the incidence of bone metastasis was not significantly different between patients with differential expression of *NOTCH2*, *NOTCH3*, and *NOTCH4* (Figures S1H–S1J) (*NOTCH1* expression is too low for analysis). These findings further implicate Jagged1, in contrast to the Notch receptors or other pathway components, as a clinically significant player in breast cancer metastasis to the bone.

Jagged1 Mediates Breast Cancer Bone Metastasis

To directly test whether Jagged1 is functionally important for breast cancer bone metastasis, we used a short-hairpin RNA (shRNA) to stably silence its expression in SCP2 and 1833 (Figure 1E), two highly bone metastatic MDA231 sublines with high expression of *JAG1* (Figure 1B). The progression of bone metastasis after intracardiac injection of tumor cells was monitored by weekly bioluminescence imaging (BLI) using a stably expressed firefly luciferase reporter. JAG1 knockdown (KD) significantly extended survival (Figure 1F) and delayed the onset of bone metastasis in mice (Figures S1K and S1L). Despite no difference at early time points, BLI analysis showed that JAG1 KD reduced the bone tumor burden by 6- to 10-fold 3 weeks after injection (Figure 1G; Figures S1M and S1N), suggesting that tumor-derived Jagged1 is necessary for efficient outgrowth of bone lesions. We confirmed that the differences in BLI measurement of bone tumor burden corresponded to those achieved by histomorphometric and X-ray analyses (Figures 1H–1J; Figure S1M–S1O). Consistent with these results, histological analysis demonstrated a 2-fold decrease in the number of tartrate-resistant acid phosphatase-positive ($TRAP^+$) osteoclasts along the bone-tumor interface of bone lesions generated by JAG1 KD cells (Figures 1K and 1L). Importantly, JAG1 KD did not alter the ability of tumor cells to proliferate in culture or as mammary tumors in mice (Figures S1P–S1R). These results support a functional role for tumor-derived Jagged1 in bone metastasis, in part by its ability to support efficient tumor outgrowth and induce osteolysis.

To determine whether enforced expression of Jagged1 is sufficient to promote bone metastasis, we overexpressed it in the mildly metastatic MDA231 subline SCP28 (Figures S2A and S2B). Mice injected with JAG1 overexpressing (OE) tumor cells had an earlier onset of bone metastasis (Figure 2A), demonstrated a significant increase in bone metastasis burden by BLI (Figure 2B), and developed severe osteolytic bone lesions as determined by X-ray and histological analysis (Figures 2C–2E). Ki67 staining of bone metastases revealed a greater number of proliferating cancer cells in the JAG1 OE group (Figure 2F). In contrast, JAG1 OE did not increase the proliferation of tumor cells in culture or as primary mammary tumors, and did not affect their invasive ability in vitro (Figures S2C–S2E). Importantly, we found that Notch pathway target genes were elevated in the tumor-associated stroma of JAG1 OE bone metastases (Figure S2F) using mouse-specific RT-PCR analysis. These findings indicate that enforced expression of Jagged1 is sufficient to promote osteolytic bone metastasis, potentially by activating the Notch pathway in the supporting bone microenvironment.

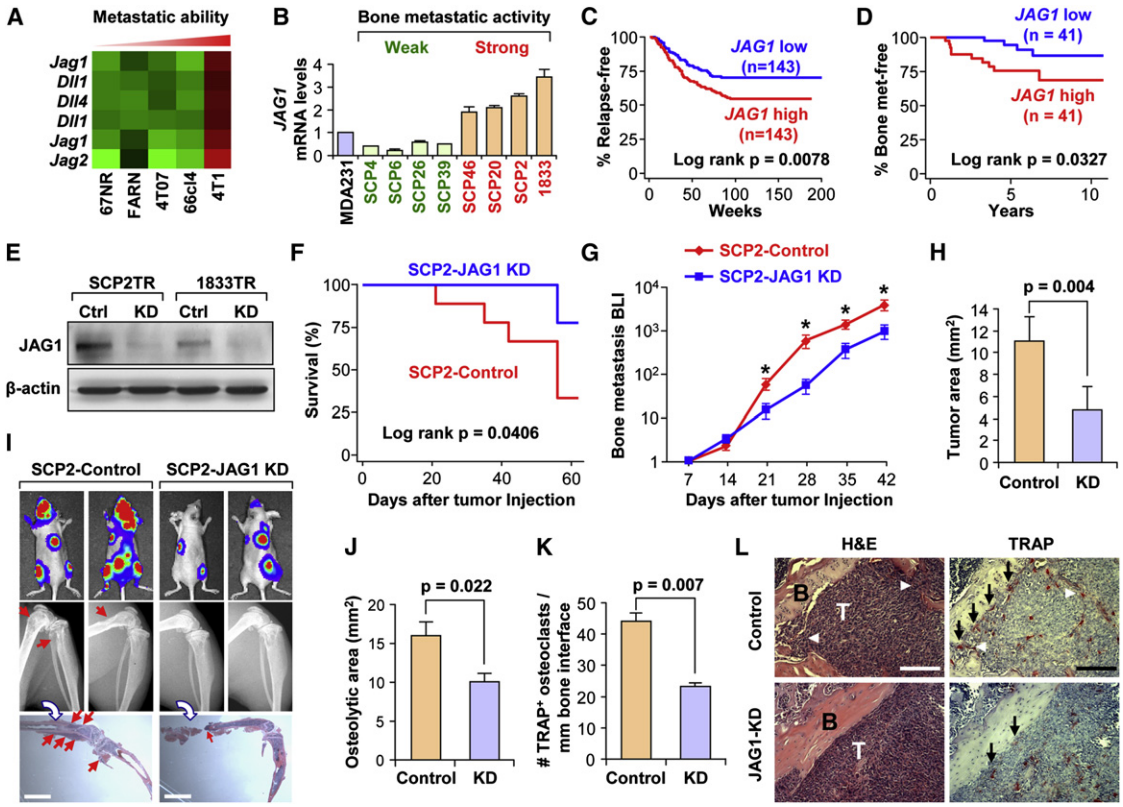

Figure 1. Tumor-Derived Jagged1 Is Associated with High Risk for Bone Metastasis and Functionally Important for Osteolytic Bone Metastasis In Vivo

(A) Heat map depicting microarray gene-expression profiling of Notch pathway ligands across the 4T1 series.

(B) mRNA expression of *JAG1* in the MDA231 cell line and its derivative sublines with distinct bone metastasis properties using qRT-PCR.

(C and D) Kaplan-Meier relapse-free survival curve of patients from the Wang data set (Wang et al., 2005) (C) and bone metastasis-free survival curve of the Minn data set (Minn et al., 2005) (D) with either low or high expression of *JAG1*.

(E) Western blot analysis showing JAGGED1 protein levels in the control and JAG1 KD SCP2 and 1833 sublines.

(F) Kaplan-Meier survival curve of mice (n = 10) inoculated with control or JAG1 KD SCP2 cells.

(G) Normalized BLI signals of bone metastases of mice (n = 10) from each experimental group. *$p < 0.05$ by Mann-Whitney test.

(H) Histomorphometric quantification of tumor area of bone lesions from each experimental group.

(I) BLI, X-ray, and histological images of bone lesions from representative mice in each experimental group. Red arrows indicate osteolytic bone lesions. Scale bar, 6 mm.

(J) Quantification of hindlimb osteolysis from mice in each experimental group using X-ray analysis.

(K) Quantification of $TRAP^+$ osteoclasts along the bone-tumor interface of metastases of mice from each experimental group.

(L) H&E and TRAP staining of bone metastasis from each experimental group. Arrows indicate $TRAP^+$ osteoclasts. Arrowheads indicate areas of overt bone destruction. Scale bar, 200 μM.

Data in the figure represent average ± SEM; p values were based on Student's t test unless otherwise indicated. See also Figure S1.

Considering the importance of the immune system in bone homeostasis (Pacifici, 2010) and the pathogenesis of bone metastasis (Xu et al., 2009), we extended our analysis to an immunocompetent mouse model for bone metastasis. Using the BALB/c-derived TM40D-MB murine breast cancer cell line (Li et al., 2008), we overexpressed mouse Jagged1 and tested its ability to promote metastasis in vivo. The results showed a significant increase in bone metastasis ability for the Jag1 OE group in both immunocompetent BALB/c and athymic nude mice (Figures S2G–S2K). These findings suggest that immune cells are unlikely to play a critical role in mediating the bone metastasis-promoting function of tumor-derived Jagged1.

Jagged1 Is Regulated by the TGFβ-SMAD Signaling Axis in Bone Metastasis

Expression of prometastatic genes is often influenced by signaling molecules present in the pathological milieu of the tumor microenvironment. To identify potential regulators of Jagged1 in the bone microenvironment, we examined the enrichment of various signaling pathway target gene sets in the transcriptome of bone metastatic tumor cells. Gene-set enrichment analysis demonstrated that TGFβ-responsive genes are significantly overrepresented among upregulated genes in bone metastatic MDA231 sublines (Figure 3A, $p = 0.0212$). Notably, *JAG1* was revealed among the 10-gene enrichment core of TGFβ responsive genes (Figure 3A), suggesting that it

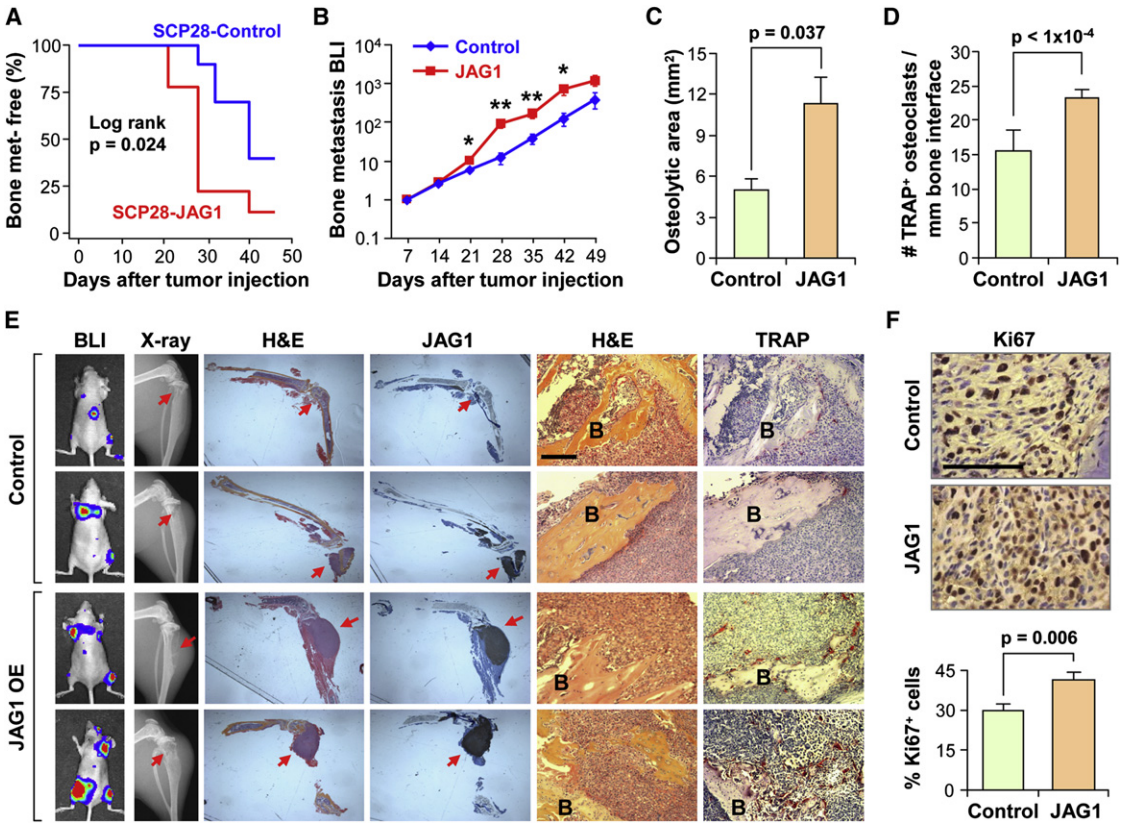

Figure 2. Enforced Expression of Jagged1 in Breast Cancer Promotes Osteolytic Bone Metastasis

(A) Kaplan-Meier bone metastasis-free survival curve of mice inoculated with control or JAG1 OE SCP28 cells (n = 10).

(B) Normalized BLI signals of bone metastases of mice from each experimental group. $^{**}p < 0.01$, $^{*}p < 0.05$.

(C) Quantification of X-ray osteolytic lesion area of hindlimbs from each experimental group.

(D) Quantification of $TRAP^{+}$ osteoclasts along the bone-tumor interface of metastases from each experimental group.

(E) BLI, X-ray, and histological (H&E and TRAP) images of bone lesions from two representative mice in each experimental group on day 42. Red arrows indicate osteolytic bone lesions in the X-ray images and tumor burden in the histological images. JAG1 images have been stained using IHC against JAGGED1. Scale bar, 200 μM.

(F) The top panel shows Ki67 immunohistochemical images of bone metastases from each experimental group. Scale bar, 200 μM. The bottom panel illustrates quantification of percent $Ki67^{+}$ tumor cells along bone-tumor interface of five distinct 20× images from each group (n = 3).

Data in the figure represent average ± SEM; p values were based on Student's t test unless otherwise indicated. See also Figure S2.

is a potential target of TGFβ in breast cancer cells during osteolytic bone metastasis. Indeed, Jagged1 is potently upregulated in several breast cancer cell lines upon TGFβ stimulation (Figure 3B; Figures S3A and S3B). TGFβ Receptor 1 kinase inhibitor treatment abolished this induction in breast cancer cells in vitro (Figures S3C and S3D) and in bone metastases in vivo (Figure S3E). Furthermore, using our previously reported SCP28 subline with conditional expression of SMAD4 (Korpal et al., 2009), we demonstrated a SMAD-dependent transcriptional regulation of *JAG1* by TGFβ signaling (Figure 3C; Figure S3F).

We next investigated whether Jagged1 is an important downstream effector of the prometastatic TGFβ-SMAD signaling pathway during bone metastasis in vivo. As previously reported, SMAD4 KD significantly inhibits the development of osteolytic bone metastasis (Kang et al., 2005) (Figures 3D–3F). We reasoned that if Jagged1 is an important TGFβ target during bone metastasis, overexpressing it in SMAD4 KD cells may partially restore their aggressive bone metastatic ability. Indeed, JAG1 OE strongly rescued the ability of SMAD4 KD tumor cells to generate osteolytic bone metastases (Figures 3D–3H). Furthermore, the reduced bone metastasis burden observed in the JAG1 KD experiments could also be explained in part by the inability of the JAG1 KD tumor cells to induce JAGGED1 expression in response to bone-derived TGFβ (Figure S3G). Taken together, these findings demonstrate that TGFβ, a well-known prometastatic cytokine, stimulates Jagged1 expression in cancer cells to promote osteolytic bone metastasis.

Jagged1 Confers a Growth Advantage by Activating Notch Signaling in Osteoblasts

Because manipulating Jagged1 expression influenced the development of bone metastasis without affecting primary tumor functions (Figures S1 and S2), it is likely that Jagged1-Notch signaling facilitates communication between tumor cells and the bone microenvironment to promote metastasis. Therefore,

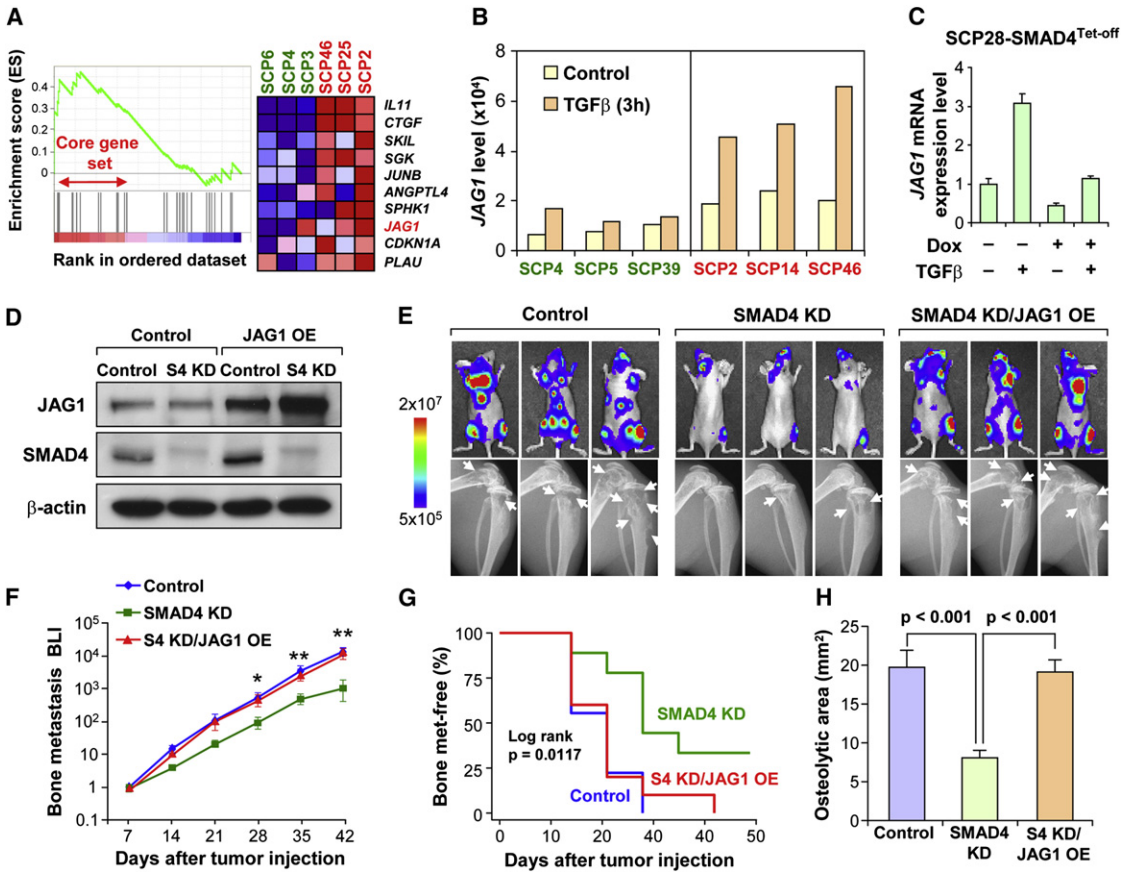

Figure 3. Jagged1 Is a Functional Target of the TGFβ-SMAD Signaling Pathway in Breast Cancer Bone Metastasis

(A) Gene-set enrichment analysis of the TGFβ-response gene set in a ranked list of differentially expressed genes in strongly versus weakly bone-metastatic MDA231 sublines (p = 0.0212). The right panel shows corresponding heat map of core TGFβ gene set with elevated expression in strongly (red) versus weakly (green) bone-metastatic MDA231 sublines.

(B) mRNA expression of *JAG1* in response to TGFβ treatment in the weakly (green) and strongly (red) bone-metastatic MDA231 sublines using previously reported microarray expression profiling data (Kang et al., 2003).

(C) qRT-PCR mRNA expression levels of *JAG1* in the SCP28 cell line with inducible (Tet-off) SMAD4 expression (Korpal et al., 2009) under the indicated TGFβ and doxycycline treatment conditions. Data represent average ± SD.

(D) Western blot analysis showing JAGGED1 and SMAD4 protein levels in the indicated cell lines with altered expression of JAGGED1 and SMAD4.

(E) BLI and X-ray images of bone lesions of three representative mice from each experimental group on day 42. White arrows indicate osteolytic lesions in the X-ray images.

(F) Normalized BLI signals of bone metastases in the hindlimbs of mice (n = 10) from each experimental group. **p < 0.01, *p < 0.05 by Student's t test.

(G) Kaplan-Meier bone metastasis-free survival curve of mice (n = 10) from each experimental group.

(H) Quantification of radiographic osteolytic lesion area of hindlimbs from each experimental group.

Student's t test p < 0.001. Data in the figure represent average ± SEM unless otherwise indicated. See also Figure S3.

we investigated the involvement of supporting bone cells, particularly osteoblasts and osteoclasts, in Jagged1-mediated bone metastasis by employing an in vitro coculture system.

We first tested the ability of tumor-derived Jagged1 to activate the Notch pathway in associated osteoblasts. When MC3T3-E1 osteoblasts expressing a Notch reporter (Zeng et al., 2005) were cocultured with JAG1 OE tumor cells, we observed a 6-fold increase in Notch activity that was abolished by the γ-secretase inhibitor (GSI) MRK-003 (Figure 4A). Moreover, osteoblasts separated by FACS from cocultured JAG1 OE GFP$^+$ tumor cells (Figures S4A and S4B) demonstrated activation of several Notch target genes that were downregulated by MRK-003 treatment (Figure 4B).

Considering the elevated proliferative index (Ki67$^+$) of JAG1 OE bone metastases (Figure 2F), we investigated whether the growth advantage was acquired via interactions with osteoblasts. We tested this by culturing GFP$^+$-luciferase labeled tumor cells over a monolayer of MC3T3-E1 osteoblasts and subsequently quantifying tumor proliferation via luciferase assay. The results showed a 2-fold increase in the number of JAG1 OE tumor cells compared to vector controls when normalized to the counts of either population cultured without osteoblasts (no coculture) (Figures 4C and 4D). Moreover, JAG1 OE tumor cells formed GFP$^+$ colonies that were 2.5-fold larger in diameter (Figure 4E). MRK-003 treatment abolished the growth advantage of JAG1 OE tumor cells in the osteoblast coculture

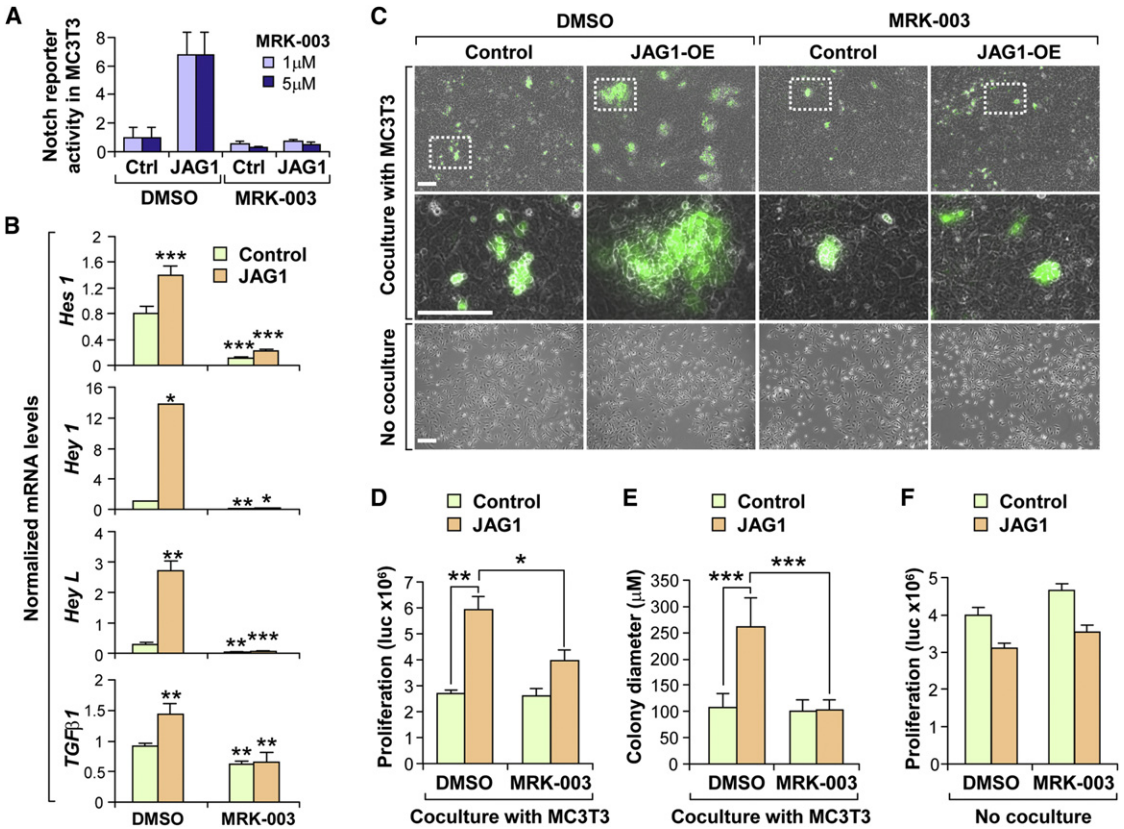

Figure 4. Jagged1-Expressing Tumor Cells Have a Growth Advantage in the Bone Microenvironment via Notch-Dependent Crosstalk with Osteoblasts

(A) Coculture between control or JAG1 OE SCP28 tumor cells and MC3T3-E1 osteoblasts transfected with a Notch reporter and treated with DMSO or MRK-003.

(B) qRT-PCR mRNA expression levels of indicated Notch target genes and *TGFβ1* in MC3T3-E1 osteoblasts that were FACS-separated from cocultures in each experimental group. *$p < 0.05$, **$p < 0.01$, ***$p < 0.001$.

(C) Representative images of cocultures from each experimental group. White boxes indicate areas shown at higher magnification in the middle row. Tumor cells cultured alone are shown in the bottom row. Scale bar, 200 μM.

(D) Quantification of tumor cells from cocultures with MC3T3-E1 from each experimental group by luciferase assay. *$p = 0.01$, **$p = 0.007$.

(E) Diameter of tumor colonies from cocultures of each experimental group. ***$p < 10^{-7}$.

(F) Quantification of tumor cells cultured alone from each experimental group.

Data in the figure represent average ± SD; p values were based on Student's t test. See also Figure S4 and Table S1.

(Figures 4C–4E and 5A) but did not affect their proliferative ability when cultured alone (Figure 4F; Table S1). These results were also confirmed in primary bone marrow osteoblast cocultures (Figures S4C and S4D). Furthermore, genetic inhibition of Notch signaling in MC3T3-E1 via siRNA-mediated silencing of *Rbpj*, an indispensable cofactor of the Notch pathway, diminished the ability of JAG1 to stimulate tumor cell proliferation in cocultures (Figure 5B). Collectively, these findings revealed that activation of the Notch pathway in osteoblasts confers a proliferative advantage to JAG1 OE tumor cells.

To identify Jagged1-regulated genes in osteoblasts that are potentially required for the enhanced tumor growth properties, we performed microarray profiling of the MC3T3-E1 cells that were FACS-separated from tumor cell cocultures (Figure S4B). Transcriptomic profiling uncovered 123 genes that were activated by at least 3-fold in MC3T3-E1 cells cocultured with JAG1 OE tumor cells relative to controls. These genes were concomitantly downregulated in the MRK-003-treated groups (Figure 5C). As expected, many well-characterized Notch targets were found among these candidate genes. We proceeded to investigate the necessity of *Hey1*, the most upregulated downstream mediator of the Notch pathway, by silencing its expression in MC3T3-E1 (Figure S4E). *Hey1* KD in MC3T3-E1 significantly diminished the coculture growth of JAG1 OE tumor cells (Figure 5E), suggesting that Hey1 is a required downstream mediator of Notch signaling in osteoblasts for promoting tumor growth.

Next, we sought to identify Notch-dependent signaling proteins secreted by osteoblasts that may potentially stimulate tumor growth. The most promising candidate from the ranked gene list was *interleukin-6* (*IL-6*) (Figure 5D) because it is implicated in the development of bone metastasis (Ara et al., 2009; de la Mata et al., 1995) and associated with poor clinical outcome in patients with breast cancer (Salgado et al., 2003). JAG1 OE cocultures demonstrated a 7-fold increase in IL-6 levels by ELISA (Figures 5F–5H). Importantly, IL-6 was selectively secreted by osteoblasts since conditioned media from

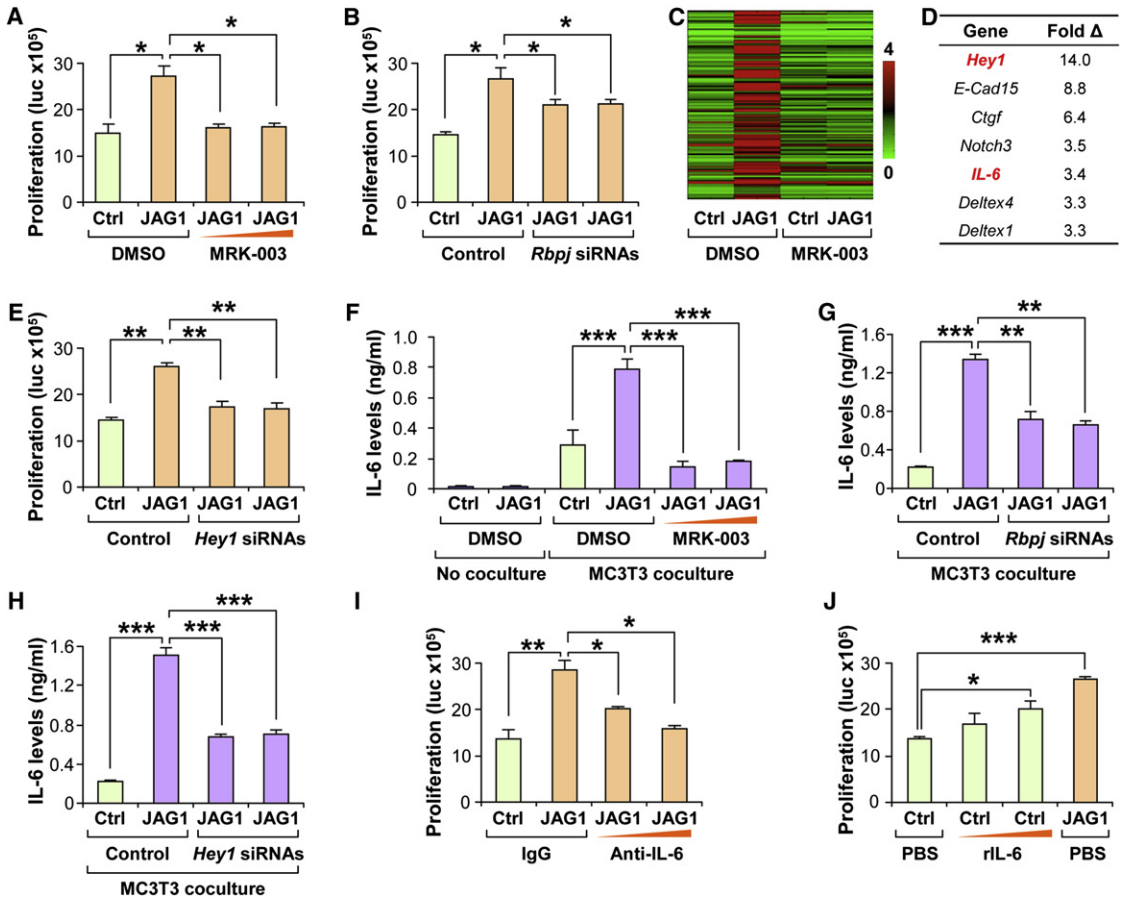

Figure 5. IL-6 Is Secreted by Osteoblasts in a Notch- and Hey1-Dependent Fashion and Stimulates the Growth of Jagged1-Expressing Tumor Cells

(A) Quantification of control or JAG1 OE tumor cells cocultured with MC3T3-E1 cells and treated with DMSO, 1 μM, or 5 μM MRK-003 by luciferase assay. *$p < 0.05$.

(B) Quantification of indicated tumor cells cocultured with MC3T3-E1 cells that were treated with *Rbpj* siRNAs by luciferase assay. *$p < 0.05$.

(C) Heat map depicting microarray gene expression profiling of MC3T3-E1 osteoblasts that were FACS-separated from cocultures of each experimental group.

(D) A list of genes with expression levels greater than 3-fold in osteoblasts cocultured with JAG1 OE tumor cells relative to controls.

(E) Quantification of indicated tumor cells cocultured with MC3T3-E1 cells that were treated with *Hey1* siRNAs by luciferase assay. **$p < 0.005$.

(F) Quantification of IL-6 levels in conditioned media of control or JAG1 OE tumor cells cultured alone or cocultured with MC3T3-E1 cells in the presence of DMSO, 1 μM, or 5 μM MRK-003 using ELISA. ***$p < 1 \times 10^{-5}$.

(G) ELISA quantification of IL-6 levels in conditioned media of indicated tumor cells cocultured with MC3T3-E1 cells treated with *Rbpj* siRNAs. **$p < 0.0005$, ***$p < 1 \times 10^{-4}$.

(H) Quantification of IL-6 levels in conditioned media of indicated tumor cells cocultured with MC3T3-E1 cells treated with *Hey1* siRNAs using ELISA. ***$p < 0.0005$.

(I) Quantification of indicated tumor cells cocultured with MC3T3-E1 cells and treated with IgG, 0.5 μg/ml, or 1.0 μg/ml anti-mouse IL-6 by luciferase assay. *$p < 0.05$, **$p = 0.007$.

(J) Quantification of indicated tumor cells cocultured with MC3T3-E1 cells and treated with PBS, 10 ng/ml, or 100 ng/ml hIL-6 by luciferase assay. *$p < 0.05$, ***$p < 1 \times 10^{-5}$.

Data in the figure represent average ± SD; p values were based on Student's t test.

tumor cells cultured alone contained negligible amounts of IL-6 (Figure 5F); this is consistent with the observation that JAG1 OE promotes tumor cell growth only in the presence of MC3T3-E1 cells. IL-6 transcription and secretion from osteoblasts were dependent on the Notch pathway, as shown by MRK-003 and *Rbpj* siRNA treatments (Figures 5F and 5G; Figure S4F). Furthermore, we validated that Hey1 regulates both mRNA and protein levels of IL-6 (Figure 5H; Figure S4G). Based on these results, we proceeded to test whether Notch-stimulated IL-6 secretion from osteoblasts was required for the enhanced tumor proliferation. Inhibition of osteoblast-derived IL-6 by a neutralizing antibody diminished the growth advantage of JAG1 OE tumor cells (Figure 5I). Conversely, stimulation of control tumor cells by rIL-6 significantly enhanced their proliferative ability (Figure 5J). These findings outline a positive feedback signaling axis by which Jagged1-Notch signaling stimulates the release of IL-6 from osteoblasts to promote tumor proliferation.

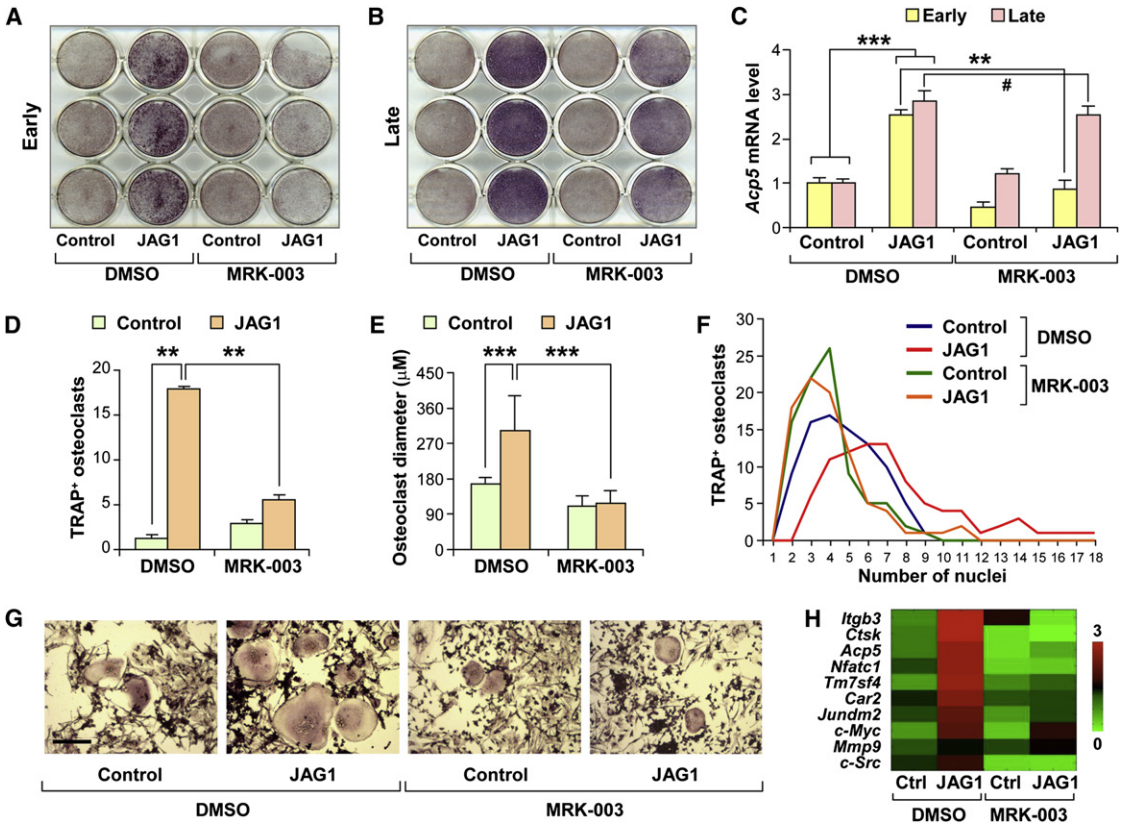

Figure 6. Jagged1-Expressing Tumor Cells Stimulate Osteoclastogenesis and Osteolytic Bone Lesions via Notch-Dependent Signaling

(A) TRAP staining of cocultures of control or JAG1 OE tumor cells with pre-osteoclast Raw 264.7 cells treated with DMSO or 1 μM MRK-003 immediately after seeding in the displayed 12-well plate (Early).

(B) TRAP staining of similar experiment as (A) except DMSO or 1 μM MRK-003 treatment was initiated 2 days after seeding (Late).

(C) qRT-PCR mRNA expression levels of mouse *Apc5* (encoding mouse TRAP) from the experimental groups described in (A) and (B). $^{**}p = 0.001$, $^{***}p < 10^{-4}$, $^{\#}p > 0.4$.

(D) Quantification of TRAP$^+$ osteoclasts from experiment (A). $^{**}p < 1 \times 10^{-4}$.

(E) Diameter of TRAP$^+$ osteoclasts from experiment (A). $^{***}p < 1 \times 10^{-7}$.

(F) Quantification of TRAP$^+$ osteoclasts with the indicated number of nuclei from experiment (A). Number of osteoclasts quantified per group is 86.

(G) Representative images of TRAP$^+$ osteoclasts from experiment (A). Scale bar, 400 μM.

(H) Heat map depicting qRT-PCR mRNA expression levels of osteoclast differentiation markers in Raw 264.7 cells that have been cocultured under the indicated conditions using mouse-specific primers.

Data in the figure represent average ± SD; p values were based Student's t test. See also Figure S5.

Tumor-Derived Jagged1 Directly Promotes Osteoclast Differentiation

The severe osteolytic phenotype observed in Jagged1-mediated bone metastases could be explained by two possible mechanisms. JAGGED1-expressing tumor cells may indirectly impact osteoclast activity by altering the expression of osteoblast-derived Rankl and Opg. Alternatively, JAG1 OE tumor cells may directly interact with pre-osteoclasts to stimulate their maturation. The first possibility was ruled out by the observation that there was no difference in mRNA and protein levels of Rankl and Opg in MC3T3-E1-tumor cell cocultures from each experimental condition (Figures S5A–S5E). Moreover, the conditioned media from these cocultures did not impact osteoclast properties (data not shown). Therefore, we proceeded to test the second possibility by directly coculturing tumor cells with pre-osteoclast Raw 264.7 cells. Strikingly, JAG1 OE cocultures showed a 15-fold increase in TRAP$^+$ osteoclasts relative to controls, whereas MRK-003 treatment essentially abolished this phenotype (Figures 6A and 6D). These findings were confirmed in primary osteoclast cocultures (Figures S5F–S5I) and by using recombinant JAGGED1 protein (rJAG1) alone, a different GSI (GSI IX), and an additional murine osteoclast precursor cell line (MOCP5) (Figures S5J–S5O). Delayed initiation of MRK-003 treatment (Late) failed to fully rescue the phenotype, as shown by *Acp5* (mouse gene encoding TRAP) mRNA levels (Figures 6B and 6C), implying that JAGGED1 facilitates an early stage in osteoclast maturation. Furthermore, TRAP$^+$ osteoclasts in JAG1 OE cocultures were significantly larger (Figures 6E and 6G) and contained more nuclei (Figure 6F), suggesting more efficient osteoclast fusion and accelerated differentiation. In contrast, cocultures treated with MRK-003 displayed smaller osteoclasts with fewer nuclei (Figures 6E–6G).

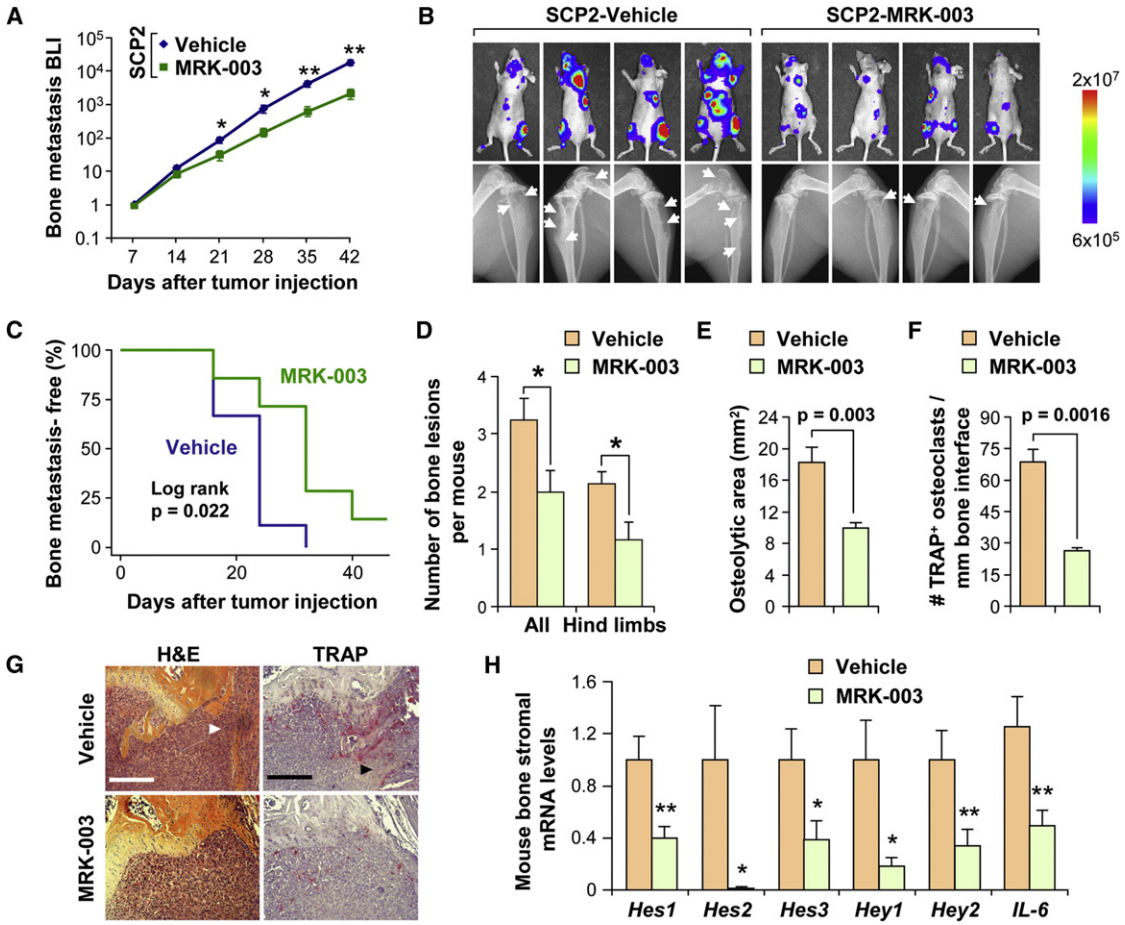

Figure 7. Disrupting the Notch Pathway with MRK-003 Reduces Osteolytic Bone Metastasis

(A) Normalized BLI signals of bone metastasis in mice (n = 10) that have been injected with SCP2 cells and treated with vehicle or MRK-003. *p < 0.05, **p < 0.005.

(B) BLI and X-ray images of bone lesions from four representative mice in each experimental group.

(C) Kaplan-Meier bone metastasis-free survival curve of mice from each experimental group.

(D) Quantification of total and hindlimb bone lesions in vehicle or MRK003-treated mice. *p < 0.05.

(E) Quantification of radiographic osteolytic lesion area of hindlimbs of mice from each experimental group.

(F) Quantification of TRAP$^+$ osteoclasts along the bone-tumor interface of metastases of mice from each experimental group.

(G) Histological (H&E and TRAP staining) analysis of bone metastases from each experimental group. Arrowheads indicate bone destruction in histological sections of vehicle mice. Scale bar, 200 μM.

(H) qRT-PCR mRNA expression of Notch target genes and mouse *IL-6* in the stromal compartment of bone metastasis from vehicle or MRK-003-treated mice using mouse-specific primers. *p < 0.005, **p < 0.001.

Data in the figure represent average ± SEM; p values were based on Student's t test unless otherwise indicated.

To further validate these findings, we profiled mRNA expression levels of osteoclast differentiation markers in Raw 264.7 cells. As anticipated, expression of several markers was elevated in the JAG1 OE cocultures and suppressed in the MRK-003-treated cocultures (Figure 6H). Taken together, these results demonstrate that JAGGED1-expressing tumor cells are capable of directly activating osteoclasts and help provide a mechanistic explanation for the severe osteolytic phenotype observed in mice.

Disruption of Notch Signaling in the Bone Microenvironment Reduces Bone Metastasis

We next asked whether MRK-003 treatment can reduce bone metastasis by targeting the supporting bone microenvironment. To this end, mice were inoculated with the aggressive bone-tropic subline SCP2, which expresses high endogenous *JAG1* levels (Figure 1B), and concomitantly treated with MRK-003. MRK-003 treatment led to a 5-fold reduction in bone metastasis burden by BLI and an approximate 10-day delay in the onset of bone metastasis (Figures 7A–7C). The number of bone lesions was also reduced in the MRK-003-treated group (Figure 7D), which was accompanied by a 2-fold reduction in X-ray lesion area (Figures 7B and 7E) and a 3-fold decrease in the number of TRAP$^+$ osteoclasts (Figures 7F and 7G). In contrast the growth rate of primary mammary tumors was not altered by MRK-003 treatment (data not shown), suggesting that direct targeting of Notch signaling in tumor cells cannot explain the reduced tumor burden in the bone metastasis experiments. We also confirmed

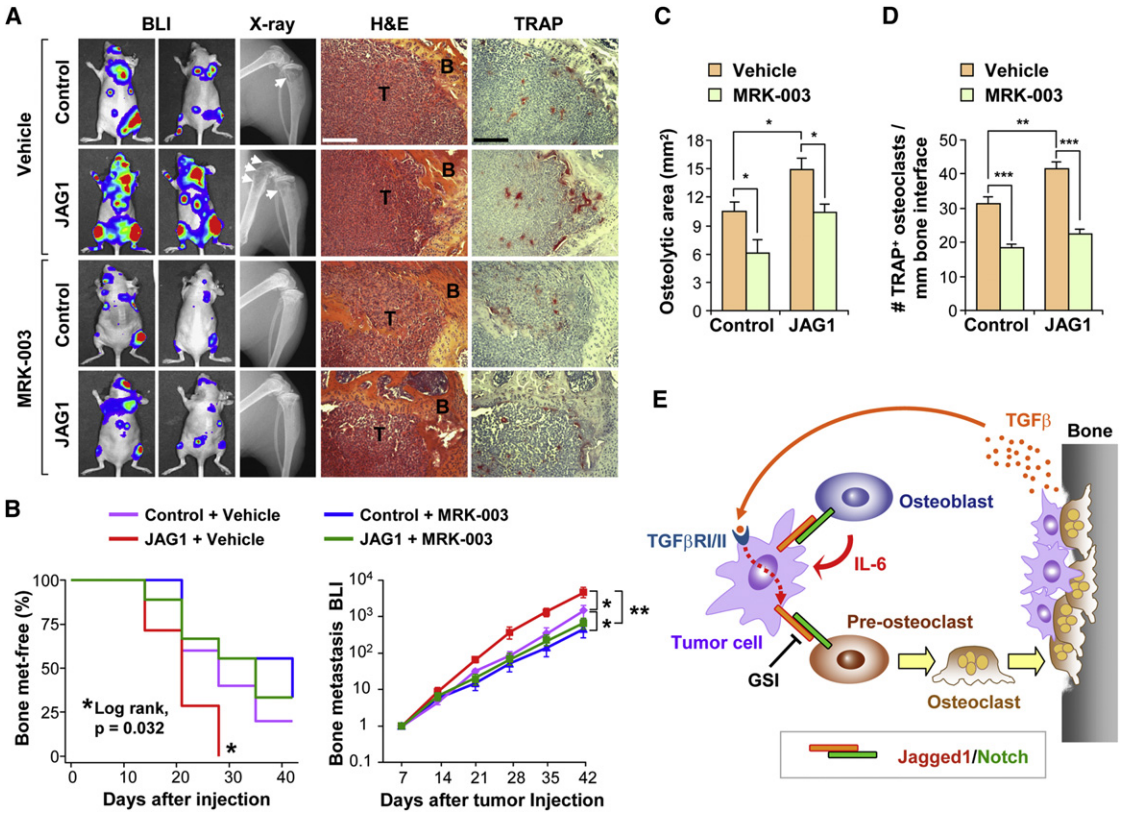

Figure 8. Disrupting the Notch Pathway with MRK-003 Reverses Jagged1-Mediated Bone Metastasis

(A) BLI, X-ray, and histological images of bone lesions from representative mice in each experimental group on day 42. Scale bar, 200 μM.

(B) The left graph shows Kaplan-Meier bone metastasis-free survival curve of mice from each experimental group over time. Log rank p = 0.032. The right graph illustrates normalized BLI signals of bone metastasis in mice inoculated with control or JAG1 OE tumor cells and treated with vehicle or MRK-003. *p < 0.05, **p < 0.01 based on repeated-measures ANOVA.

(C) Quantification of radiographic osteolytic lesion area of mice hindlimbs from each experimental group. *p < 0.05 by Student's t test.

(D) Quantification of $TRAP^+$ osteoclasts along the bone-tumor interface of metastases from each experimental group. **p < 0.005, ***p < 1×10^{-4} by Student's t test.

(E) Schematic depicting tumor-stroma interactions of JAGGED1-expressing tumor cells with the bone microenvironment. See text for details.

Data in the figure represent average ± SEM.

that MRK-003 treatment disrupted Notch signaling in the stromal compartment of bone metastases since expression levels of several Notch target genes, as well as *IL-6*, were significantly reduced in the stromal compartment of MRK-003-treated bone metastases, as measured by species-specific qRT-PCR (Figure 7H).

We further tested whether MRK-003 treatment could reverse the severe bone metastasis phenotype induced by JAG1 OE. The significant increase in bone metastasis observed in the JAG1 OE group was reduced by more than 6-fold when the mice were treated with MRK-003, decreasing the tumor signal to levels found in the control group (Figures 8A–8C). Mirroring these changes in bone tumor dynamics, osteolysis was also reduced in MRK-003-treated mice (Figures 8B–8D). Overall, these preclinical studies confirm that the severe osteolytic bone metastasis phenotype mediated by Jagged1-expressing breast cancer is dependent on stromal Notch activation and is, therefore, susceptible to pharmacological inhibition of the Notch pathway in the bone microenvironment.

DISCUSSION

In this study we show that elevated expression of Jagged1 in breast cancer cells promotes bone metastasis by activating the Notch pathway in supporting bone cells (Figure 8E). Jagged1 is overexpressed in bone metastatic tumor cells and is further activated by the bone-derived cytokine TGFβ during osteolytic bone metastasis. Jagged1-expressing tumor cells acquire a growth advantage in the bone microenvironment by stimulating the release of IL-6 from osteoblasts and exacerbate osteolytic lesions by directly activating osteoclast maturation. Importantly, GSI treatment reversed these prometastatic functions of Jagged1 by disrupting the Notch pathway in associated bone cells. Our findings support a distinct paradigm for the involvement of Notch signaling in the progression of breast cancer.

Notch Activation in Tumor versus Stroma

The majority of studies that implicate Notch signaling in breast cancer progression investigate its activation in tumor cells. The

first evidence that Notch plays a role in breast cancer surfaced from mouse mammary tumor virus studies in which tumor development frequently resulted from the expression of a truncated, constitutively active form of the Notch receptor (Jhappan et al., 1992). However, it is important to note that mutations that lead to truncated forms of the Notch receptors are rare in human solid tumor malignancies. Our investigation demonstrated that the Notch pathway receptors and select downstream targets are not associated with breast cancer progression. In contrast, we revealed that elevated expression of Notch pathway ligands is associated with metastatic ability of breast cancer cells and, furthermore, showed that high expression of *JAG1* in particular correlates with breast cancer bone metastasis in patient samples. Many independent studies have also supported an association between Notch pathway ligands and human cancer progression (Dickson et al., 2007; Santagata et al., 2004). Moreover, gene expression analysis of 58 human breast cancer metastasis samples revealed *JAG1* as one of 17 cytokine/ligand genes overexpressed in bone metastasis compared to liver, brain, and lung metastasis, implicating a potential organ-specific role for tumor-derived Jagged1 in metastatic colonization of the bone (Zhang et al., 2009). Despite the existence of these correlative relationships, little progress has been previously made regarding the precise mechanism underlying the involvement of Notch pathway ligands in breast cancer metastasis.

Notch Signaling in the Tumor-Associated Stroma

There is emerging evidence that activation of developmental signaling pathways in the tumor-associated stroma facilitates cancer progression (Sethi and Kang, 2011). A recent study revealed that aberrant activation of the sonic hedgehog (SHH) signaling pathway in the tumor-associated stromal microenvironment supported primary tumor growth in xenografts (Yauch et al., 2008). Our study shows that tumor-derived Jagged1 can facilitate outgrowth of bone metastases by activating the Notch signaling pathway in two major residential cell types specific to the bone microenvironment. Importantly, bone-specific cells can also express Jagged1 (Weber and Calvi, 2010; Weber et al., 2006) and regulate hematopoietic stem cell niches via Notch signaling (Calvi et al., 2003). Therefore, it is conceivable that tumor-derived Jagged1 may be capable of stimulating the expansion of hematopoietic niches, which may potentially support the colonization of tumor cells in the bone microenvironment. Such a scenario warrants further investigation, as we do not evaluate the involvement of other stromal cells, including endothelial cells and hematopoietic stem cells, in Jagged1-mediated bone metastasis.

Activation of the Notch pathway in murine stromal cells has been reported to promote osteoblast differentiation (Nobta et al., 2005; Tezuka et al., 2002). Conversely, loss- and gain-of-function experiments in mice demonstrated that Notch signaling directly inhibits osteoblast differentiation (Engin et al., 2008; Hilton et al., 2008). These studies suggest a context-dependent role of Notch signaling in osteoblast function (Zanotti and Canalis, 2010). Some of our gene expression analysis (*Runx2* and *Osx*) pointed to a very modest increase of osteoblast differentiation in JAG1 OE cancer cell cocultures (Figure S4C). However, unlike the strong impact of Jagged1 on osteoclast maturation, it was unclear whether the modest differentiation of osteoblasts directly contributed to the prometastasis functions of Jagged1. On the other hand, our coculture studies revealed that Jagged1 induces the expression and secretion of IL-6 from osteoblasts via activation of the Notch-signaling cascade, in turn conferring an osteoblast-dependent proliferative advantage to tumor cells. IL-6 is associated with a poor prognosis in breast cancer (Salgado et al., 2003) and is capable of supporting tumor growth in the bone microenvironment (Sasser et al., 2007). In neuroblastoma and multiple myeloma, stromal-derived IL-6 has been shown to be an important mediator between cancer cells and the bone microenvironment by supporting tumor survival and affecting osteoclast differentiation, respectively (Ara et al., 2009; Mitsiades et al., 2006). In our present study the pathological role of IL-6 is further extended to its involvement in Jagged1-mediated bone metastasis via an osteoblast-dependent positive feedback mechanism.

The Notch pathway is also an important determinant of osteoclast maturation and function in the physiological setting (Yamada et al., 2003). Transgenic mouse models have shown that functional loss of particular Notch isoforms in pre-osteoclasts can increase osteoclastogenesis (Bai et al., 2008). Conversely, Jagged1-mediated Notch signaling has also been shown to promote osteoclast activation (Fukushima et al., 2008). These controversial results suggest, once again, a potential context-dependent role for the Notch pathway in osteoclastogenesis. However, to our knowledge, the role of Notch signaling in regulating osteoclast function in pathological conditions such as bone metastasis has not been delineated. The severe osteolytic pathology in mice inoculated with JAG1 OE tumor cells pointed to an effect of tumor-derived Jagged1 on osteoclastogenesis. We found that Jagged1 can enhance osteoclastogenesis in primary bone marrow cell cocultures. The functional role of Jagged1 as a direct mediator of osteoclast differentiation was further validated using tumor cell cocultures with two different osteoclast cell lines and the application of pure recombinant Jagged1. Not only did we observe a greater number of osteoclasts in JAG1 OE cocultures, we also noticed a more differentiated population that was unequivocally confirmed by transcriptional profiling of osteoclast differentiation markers. Overall, our in vivo and in vitro studies demonstrated a direct and strong impact of Jagged1 in promoting osteoclastogenesis and bone destruction.

Jagged1 as a Central Mediator of Notch-TGFβ Signaling Crosstalk in Bone Metastasis

The important contribution of bone-derived TGFβ during osteolytic bone metastasis is well established. Bone is a rich reservoir of TGFβ, which is released into the bone microenvironment during osteolytic bone metastasis. Genetic or pharmacological disruption of TGFβ signaling potently reduces the development of bone metastasis, emphasizing the importance of the TGFβ pathway in supporting the bone metastatic ability of tumor cells (Korpal et al., 2009; Yin et al., 1999). However, the functional downstream targets of the TGFβ-SMAD pathway in bone metastasis remain poorly defined. Here, we show that Jagged1 is a SMAD-dependent target of TGFβ in breast cancer bone metastasis and that reestablishing JAGGED1 expression in a SMAD4 KD background restores the potency of tumor cells to generate osteolytic bone metastasis. Thus, Jagged1 may mediate

a positive feedback in response to bone-derived TGFβ during the vicious cycle of osteolytic bone metastasis. Intriguingly, we also observed an upregulation of the *Tgfβ1* transcript in osteoblasts and osteoclasts upon activation of the Notch pathway (Figure 4B; Figure S5G). However, administration of a neutralizing antibody preventing the feedback of TGFβ on JAG1 OE tumor cells in osteoblast cocultures did not significantly alter their growth properties (data not shown). Collectively, these studies suggest that the release of bone-derived TGFβ in response to osteolysis, as opposed to de novo expression of osteoblast-derived TGFβ in response to Notch activation, is likely to be more critical in the pathogenesis of Jagged1-mediated bone metastasis. The Notch and TGFβ-signaling pathways have been shown to converge in diverse contexts such as epithelial to mesenchymal transition (Zavadil et al., 2004) and the pathogenesis of glomerular disease (Niranjan et al., 2008). Our results show that these two pathways once again link up to constitute a potent positive feedback loop between tumor cells and the bone microenvironment to promote osteolytic bone metastasis.

GSIs as Therapy against Breast Cancer Bone Metastasis

Disruption of the Notch pathway has been achieved through pharmacological inhibition of γ-secretase, the enzymatic complex that mediates the final cleavage of the Notch receptor leading to release of its transcription-activating intracellular domain. These pharmacological agents, known as GSIs, are gaining recognition as potential anticancer agents (Rizzo et al., 2008). However, it has not been definitively determined whether cancer progression is impeded by disrupting Notch signaling in the tumor cells or the associated stromal microenvironment. Moreover, a few studies have revealed a subset of cancer cell lines that are resistant to GSI treatment. Consistently, our proliferation assays and primary tumor xenografts of MDA231 sublines revealed no difference between control and MRK-003-treated groups, particularly at relatively low concentrations that were sufficient to inhibit the Notch pathway in bone-specific cells. These findings were supported by another study in which a panel of six breast cancer cell lines, including MDA231, were treated with three distinct GSIs, and no effect on proliferation/survival was observed for two of the compounds, whereas the third elicited cytostasis at concentrations similar to that of a proteosome inhibitor, suggesting nonspecific γ-secretase-independent effects (Han et al., 2009). We used an extensive series of experiments to show that MRK-003 disrupts bone-specific tumor functions by inhibiting the Jagged1-Notch mediated crosstalk between tumor cells and supporting bone cells. These findings support the application of GSIs as therapy against bone metastasis, most probably at a dosage that would circumvent drug-associated toxicities such as gastrointestinal irritation.

In conclusion we have revealed an important stroma-dependent mechanism for the Notch ligand Jagged1 in promoting breast cancer metastasis to the bone. Our study also revealed the convergence of two developmentally conserved signaling pathways—TGFβ and Notch—in the pathological crosstalk between tumor cells, bone-specific cells, and the bone matrix during breast cancer bone metastasis. Importantly, we have provided robust preclinical evidence for GSIs as therapeutic agents against bone metastasis by targeting the tumor-associated stroma.

EXPERIMENTAL PROCEDURES

Tumor Xenografts and Bioluminescence Analysis

All procedures involving mice and experimental protocols were approved by Institutional Animal Care and Use Committee (IACUC) of Princeton University. For bone metastasis studies, 10^5 tumor cells were injected into the left cardiac ventricle of anesthetized female athymic Ncr-nu/nu or BALB/c mice. Development of metastases was monitored by BLI. Anesthetized mice were retro-orbitally injected with 75 mg/kg D-Luciferin. Bioluminescence images were acquired with a Xenogen IVIS 200 Imaging System. Analysis was performed with Living Image software by measuring photon flux in the hindlimbs of mice. Data were normalized to the signal on day 7. Bone metastasis-free survival curves represent the time point at which each mouse developed bone metastasis by threshold BLI signals in the hindlimbs. For the orthotopic xenograft model, mammary fat pad injections and primary tumor size measurements were performed following the procedure described previously (Minn et al., 2005).

Osteoblast Coculture, Gene Expression, and Microarray Analysis

MC3T3-E1 cells were seeded at 2×10^5 cells/well in 12-well plates. After confluence was achieved, luciferase/GFP-labeled (GFP^+) control and JAG1 OE cells were added at 1×10^4 cells/well in triplicate and treated with DMSO or 1 μM MRK-003. Media supplemented with appropriate drugs were changed every 2 days. After 6 days the coculture was subjected to a luciferase assay to selectively quantify the number of tumor cells. These values were normalized against luciferase quantification of 12-well plates seeded with tumor cells alone.

For gene expression analysis, MC3T3-E1 cells were grown to confluence in 10 cm culture dishes. The 2×10^5 GFP^+ control or JAG1 OE cells were seeded onto the plate in osteoblast media. Cell sorting was performed to purify the GFP-negative MC3T3-E1 osteoblasts 5 days after initial coculture. RNA from FACS-separated MC3T3-E1 cells was collected in RLT lysis buffer, extracted with RNeasy Mini Kit (QIAGEN), and subjected to quantitative RT-PCR.

For microarray analysis the quality of the FACS-separated MC3T3-E1 RNA samples was monitored using the 2100 bioanalyzer (Agilent) before gene expression profiling with the Agilent mouse 4×44k microarrays. To find genes regulated by JAGGED1 and MRK-003 in osteoblasts, expression data of MC3T3-E1 under the indicated coculture and treatment conditions were generated and normalized by the array median, and probes were filtered by the expression levels. Probes with >2-fold changes in MC3T3-E1 cells cocultured with JAG1 OE tumor cells relative to vector-control tumor cells were identified as the regulated genes.

Osteoclastogenesis Coculture Assay

After seeding 5×10^4 control or JAG1 OE tumor cells/well into 12-well plates, murine pre-osteoclast Raw 264.7 (2×10^5 cells/well) or MOCP5 (5×10^5 cells/well) cells in media containing 30 ng/ml RANKL and DMSO or 1 μM MRK-003 were added the next day. Media were changed every 2 days. TRAP staining was performed on day 6 using a leukocyte acid phosphatase kit (Sigma). $TRAP^+$-multinucleated cells were scored as mature osteoclasts. The number of nuclei per osteoclast was quantified using TRAP-stained images. Mouse-specific qRT-PCR primers were used to selectively quantify Raw264.7 osteoclast gene expression levels after 6 days of coculture.

For primary osteoclast coculture assays, bone marrow cells were flushed out from femora and tibiae of 4- to 6-week-old wild-type FVB mice and plated in basal culture medium overnight. The next day, nonadherent cells were added at 1×10^6/well to 12-well plates that were previously seeded with either control or JAG1 OE tumor cells supplemented with 50 ng/ml RANKL and 50 ng/ml M-CSF. Medium was changed every 3 days. TRAP staining and scoring were performed on days 10–12 as described above.

Statistical Analysis

Results are presented as average ± standard deviation (SD) or as average ± standard error of the mean (SEM), as indicated in figure legends. Comparisons between Kaplan-Meier curves were performed using the log rank test. BLI signals were analyzed by unpaired, two-sided, independent Student's t test without equal variance assumption, nonparametric Mann-Whitney test, or

ANOVA. All other comparisons were analyzed by unpaired, two-sided, independent Student's t test without equal variance assumption.

ACCESSION NUMBERS

Microarray data reported herein have been deposited at the NCBI Gene Expression Omnibus (http://www.ncbi.nlm.nih.gov/geo/) with the accession code GSE20517.

SUPPLEMENTAL INFORMATION

Supplemental Information includes Supplemental Experimental Procedures, five figures, and one table and can be found with this article online at doi:10.1016/j.ccr.2010.12.022.

ACKNOWLEDGMENTS

This work is dedicated to the memory of our colleague G.R. Mundy, whose work inspired us to venture into the field of bone metastasis research. We thank M. Korpal, Y. Wei, X. Lu, M. Blanco, E. Mu, K. Golden, L. Cong, P. Bisher, C. DeCoste, S. Ganesan, M. Tetruashvily, D. Quek, Y. Min, H. Zheng, and other members of the laboratory for technical assistance and discussions, F. Miller for the 4T1 series cell lines, M. Zhang for TM40D-MB cell line, and C.-Y. Wang for the PGA-986-1 Notch reporter plasmid. This work was funded by grants from the Brewster Foundation, Department of Defense (BC051647), New Jersey Commission on Cancer Research (NJCCR), National Institutes of Health (R01CA134519), American Cancer Society, and Merck. N.S. is a recipient of a NJCCR predoctoral fellowship, and Y.K. is an investigator of the Champalimaud Metastasis Program at Princeton University. X.D. and C.G.W. are employees and shareholders of Merck & Co., Inc.

Received: March 8, 2010
Revised: August 17, 2010
Accepted: November 10, 2010
Published online: February 3, 2011

REFERENCES

Ara, T., Song, L., Shimada, H., Keshelava, N., Russell, H.V., Metelitsa, L.S., Groshen, S.G., Seeger, R.C., and DeClerck, Y.A. (2009). Interleukin-6 in the bone marrow microenvironment promotes the growth and survival of neuroblastoma cells. Cancer Res. *69*, 329–337.

Artavanis-Tsakonas, S., Rand, M.D., and Lake, R.J. (1999). Notch signaling: cell fate control and signal integration in development. Science *284*, 770–776.

Aslakson, C.J., and Miller, F.R. (1992). Selective events in the metastatic process defined by analysis of the sequential dissemination of subpopulations of a mouse mammary tumor. Cancer Res. *52*, 1399–1405.

Bai, S., Kopan, R., Zou, W., Hilton, M.J., Ong, C.T., Long, F., Ross, F.P., and Teitelbaum, S.L. (2008). NOTCH1 regulates osteoclastogenesis directly in osteoclast precursors and indirectly via osteoblast lineage cells. J. Biol. Chem. *283*, 6509–6518.

Calvi, L.M., Adams, G.B., Weibrecht, K.W., Weber, J.M., Olson, D.P., Knight, M.C., Martin, R.P., Schipani, E., Divieti, P., Bringhurst, F.R., et al. (2003). Osteoblastic cells regulate the haematopoietic stem cell niche. Nature *425*, 841–846.

de la Mata, J., Uy, H.L., Guise, T.A., Story, B., Boyce, B.F., Mundy, G.R., and Roodman, G.D. (1995). Interleukin-6 enhances hypercalcemia and bone resorption mediated by parathyroid hormone-related protein in vivo. J. Clin. Invest. *95*, 2846–2852.

Dickson, B.C., Mulligan, A.M., Zhang, H., Lockwood, G., O'Malley, F.P., Egan, S.E., and Reedijk, M. (2007). High-level JAG1 mRNA and protein predict poor outcome in breast cancer. Mod. Pathol. *20*, 685–693.

Engin, F., Yao, Z., Yang, T., Zhou, G., Bertin, T., Jiang, M.M., Chen, Y., Wang, L., Zheng, H., Sutton, R.E., et al. (2008). Dimorphic effects of Notch signaling in bone homeostasis. Nat. Med. *14*, 299–305.

Fukushima, H., Nakao, A., Okamoto, F., Shin, M., Kajiya, H., Sakano, S., Bigas, A., Jimi, E., and Okabe, K. (2008). The association of Notch2 and NF-kappaB accelerates RANKL-induced osteoclastogenesis. Mol. Cell. Biol. *28*, 6402–6412.

Guise, T.A., Yin, J.J., Taylor, S.D., Kumagai, Y., Dallas, M., Boyce, B.F., Yoneda, T., and Mundy, G.R. (1996). Evidence for a causal role of parathyroid hormone-related protein in the pathogenesis of human breast cancer-mediated osteolysis. J. Clin. Invest. *98*, 1544–1549.

Han, J., Ma, I., Hendzel, M.J., and Allalunis-Turner, J. (2009). The cytotoxicity of gamma-secretase inhibitor I to breast cancer cells is mediated by proteasome inhibition, not by gamma-secretase inhibition. Breast Cancer Res. *11*, R57.

Hilton, M.J., Tu, X., Wu, X., Bai, S., Zhao, H., Kobayashi, T., Kronenberg, H.M., Teitelbaum, S.L., Ross, F.P., Kopan, R., and Long, F. (2008). Notch signaling maintains bone marrow mesenchymal progenitors by suppressing osteoblast differentiation. Nat. Med. *14*, 306–314.

Jhappan, C., Gallahan, D., Stahle, C., Chu, E., Smith, G.H., Merlino, G., and Callahan, R. (1992). Expression of an activated Notch-related int-3 transgene interferes with cell differentiation and induces neoplastic transformation in mammary and salivary glands. Genes Dev. *6*, 345–355.

Kang, Y., Siegel, P.M., Shu, W., Drobnjak, M., Kakonen, S.M., Cordon-Cardo, C., Guise, T.A., and Massague, J. (2003). A multigenic program mediating breast cancer metastasis to bone. Cancer Cell *3*, 537–549.

Kang, Y., He, W., Tulley, S., Gupta, G.P., Serganova, I., Chen, C.R., Manova-Todorova, K., Blasberg, R., Gerald, W.L., and Massague, J. (2005). Breast cancer bone metastasis mediated by the Smad tumor suppressor pathway. Proc. Natl. Acad. Sci. USA *102*, 13909–13914.

Kopan, R., and Ilagan, M.X. (2009). The canonical Notch signaling pathway: unfolding the activation mechanism. Cell *137*, 216–233.

Korpal, M., Yan, J., Lu, X., Xu, S., Lerit, D.A., and Kang, Y. (2009). Imaging transforming growth factor-beta signaling dynamics and therapeutic response in breast cancer bone metastasis. Nat. Med. *15*, 960–966.

Lelekakis, M., Moseley, J.M., Martin, T.J., Hards, D., Williams, E., Ho, P., Lowen, D., Javni, J., Miller, F.R., Slavin, J., and Anderson, R.L. (1999). A novel orthotopic model of breast cancer metastasis to bone. Clin. Exp. Metastasis *17*, 163–170.

Leong, K.G., Niessen, K., Kulic, I., Raouf, A., Eaves, C., Pollet, I., and Karsan, A. (2007). Jagged1-mediated Notch activation induces epithelial-to-mesenchymal transition through Slug-induced repression of E-cadherin. J. Exp. Med. *204*, 2935–2948.

Li, Z., Schem, C., Shi, Y.H., Medina, D., and Zhang, M. (2008). Increased COX2 expression enhances tumor-induced osteoclastic lesions in breast cancer bone metastasis. Clin. Exp. Metastasis *25*, 389–400.

Minn, A.J., Gupta, G.P., Siegel, P.M., Bos, P.D., Shu, W., Giri, D.D., Viale, A., Olshen, A.B., Gerald, W.L., and Massague, J. (2005). Genes that mediate breast cancer metastasis to lung. Nature *436*, 518–524.

Mitsiades, C.S., Mitsiades, N.S., Munshi, N.C., Richardson, P.G., and Anderson, K.C. (2006). The role of the bone microenvironment in the pathophysiology and therapeutic management of multiple myeloma: interplay of growth factors, their receptors and stromal interactions. Eur. J. Cancer *42*, 1564–1573.

Mundy, G.R. (2002). Metastasis to bone: causes, consequences and therapeutic opportunities. Nat. Rev. Cancer *2*, 584–593.

Niranjan, T., Bielesz, B., Gruenwald, A., Ponda, M.P., Kopp, J.B., Thomas, D.B., and Susztak, K. (2008). The Notch pathway in podocytes plays a role in the development of glomerular disease. Nat. Med. *14*, 290–298.

Nobta, M., Tsukazaki, T., Shibata, Y., Xin, C., Moriishi, T., Sakano, S., Shindo, H., and Yamaguchi, A. (2005). Critical regulation of bone morphogenetic protein-induced osteoblastic differentiation by Delta1/Jagged1-activated Notch1 signaling. J. Biol. Chem. *280*, 15842–15848.

Pacifici, R. (2010). The immune system and bone. Arch. Biochem. Biophys. *503*, 41–53.

Reedijk, M., Odorcic, S., Chang, L., Zhang, H., Miller, N., McCready, D.R., Lockwood, G., and Egan, S.E. (2005). High-level coexpression of JAG1 and

NOTCH1 is observed in human breast cancer and is associated with poor overall survival. Cancer Res. *65*, 8530–8537.

Rizzo, P., Osipo, C., Foreman, K., Golde, T., Osborne, B., and Miele, L. (2008). Rational targeting of Notch signaling in cancer. Oncogene *27*, 5124–5131.

Salgado, R., Junius, S., Benoy, I., Van Dam, P., Vermeulen, P., Van Marck, E., Huget, P., and Dirix, L.Y. (2003). Circulating interleukin-6 predicts survival in patients with metastatic breast cancer. Int. J. Cancer *103*, 642–646.

Santagata, S., Demichelis, F., Riva, A., Varambally, S., Hofer, M.D., Kutok, J.L., Kim, R., Tang, J., Montie, J.E., Chinnaiyan, A.M., et al. (2004). JAGGED1 expression is associated with prostate cancer metastasis and recurrence. Cancer Res. *64*, 6854–6857.

Sasser, A.K., Sullivan, N.J., Studebaker, A.W., Hendey, L.F., Axel, A.E., and Hall, B.M. (2007). Interleukin-6 is a potent growth factor for ER-alpha-positive human breast cancer. FASEB J. *21*, 3763–3770.

Sethi, N., and Kang, Y. (2011). Dysregulation of developmental pathways in bone metastasis. Bone *48*, 16–22.

Tezuka, K., Yasuda, M., Watanabe, N., Morimura, N., Kuroda, K., Miyatani, S., and Hozumi, N. (2002). Stimulation of osteoblastic cell differentiation by Notch. J. Bone Miner. Res. *17*, 231–239.

Wang, Y., Klijn, J.G., Zhang, Y., Sieuwerts, A.M., Look, M.P., Yang, F., Talantov, D., Timmermans, M., Meijer-van Gelder, M.E., Yu, J., et al. (2005). Gene-expression profiles to predict distant metastasis of lymph-node-negative primary breast cancer. Lancet *365*, 671–679.

Wang, Z., Banerjee, S., Li, Y., Rahman, K.M., Zhang, Y., and Sarkar, F.H. (2006). Down-regulation of notch-1 inhibits invasion by inactivation of nuclear factor-kappaB, vascular endothelial growth factor, and matrix metalloproteinase-9 in pancreatic cancer cells. Cancer Res. *66*, 2778–2784.

Weber, J.M., and Calvi, L.M. (2010). Notch signaling and the bone marrow hematopoietic stem cell niche. Bone *46*, 281–285.

Weber, J.M., Forsythe, S.R., Christianson, C.A., Frisch, B.J., Gigliotti, B.J., Jordan, C.T., Milner, L.A., Guzman, M.L., and Calvi, L.M. (2006). Parathyroid hormone stimulates expression of the Notch ligand Jagged1 in osteoblastic cells. Bone *39*, 485–493.

Xu, Z., Hurchla, M.A., Deng, H., Uluckan, O., Bu, F., Berdy, A., Eagleton, M.C., Heller, E.A., Floyd, D.H., Dirksen, W.P., et al. (2009). Interferon-gamma targets cancer cells and osteoclasts to prevent tumor-associated bone loss and bone metastases. J. Biol. Chem. *284*, 4658–4666.

Yamada, T., Yamazaki, H., Yamane, T., Yoshino, M., Okuyama, H., Tsuneto, M., Kurino, T., Hayashi, S., and Sakano, S. (2003). Regulation of osteoclast development by Notch signaling directed to osteoclast precursors and through stromal cells. Blood *101*, 2227–2234.

Yauch, R.L., Gould, S.E., Scales, S.J., Tang, T., Tian, H., Ahn, C.P., Marshall, D., Fu, L., Januario, T., Kallop, D., et al. (2008). A paracrine requirement for hedgehog signalling in cancer. Nature *455*, 406–410.

Yin, J.J., Selander, K., Chirgwin, J.M., Dallas, M., Grubbs, B.G., Wieser, R., Massague, J., Mundy, G.R., and Guise, T.A. (1999). TGF-beta signaling blockade inhibits PTHrP secretion by breast cancer cells and bone metastases development. J. Clin. Invest. *103*, 197–206.

Zanotti, S., and Canalis, E. (2010). Notch and the skeleton. Mol. Cell. Biol. *30*, 886–896.

Zavadil, J., Cermak, L., Soto-Nieves, N., and Bottinger, E.P. (2004). Integration of TGF-beta/Smad and Jagged1/Notch signalling in epithelial-to-mesenchymal transition. EMBO J. *23*, 1155–1165.

Zeng, Q., Li, S., Chepeha, D.B., Giordano, T.J., Li, J., Zhang, H., Polverini, P.J., Nor, J., Kitajewski, J., and Wang, C.Y. (2005). Crosstalk between tumor and endothelial cells promotes tumor angiogenesis by MAPK activation of Notch signaling. Cancer Cell *8*, 13–23.

Zhang, X.H., Wang, Q., Gerald, W., Hudis, C.A., Norton, L., Smid, M., Foekens, J.A., and Massague, J. (2009). Latent bone metastasis in breast cancer tied to Src-dependent survival signals. Cancer Cell *16*, 67–78.